Adsorption 11: 133–138, 2005

Capillary Phenomena in the Framework of the Two-Dimensional Density Functional Theory

EUGENE A. USTINOV
St Petersburg State Technological Institute. 26 Moskovsky Prospect, St Petersburg, 190013, Russia

DUONG D. DO*
Department of Chemical Engineering, University of Queensland, St Lucia, QLD 4072, Australia
duongd@cheque.uq.edu.au

Abstract. We present results of application of the density functional theory (DFT) to adsorption and desorption in finite and infinite cylindrical pores accounting for the density distribution in radial and axial directions. Capillary condensation via formation of bridges is considered using canonical and grand canonical versions of the 2D DFT. The potential barrier of nucleation is determined as a function of the bulk pressure and the pore diameter. In the framework of the conventional assumptions on intermolecular interactions both 1D and 2D DFT versions lead to the same results and confirm the classical scenario of condensation and evaporation: the condensation occurs at the vapor-like spinodal point, and the evaporation corresponds to the equilibrium transition pressure. The analysis of experimental data on argon and nitrogen adsorption on MCM-41 samples seems to not completely corroborate this scenario, with adsorption branch being better described by the equilibrium pressure – diameter dependence. This points to the necessity of the further development of basic representations on the hysteresis phenomena.

Keywords: adsorption, cylindrical pore, density functional theory, capillary condensation, nucleation

Introduction

In the last decades a significant progress was achieved to provide deeper insight of the adsorption mechanism in micro and mesoporous adsorbents using numerical experiments (Suzuki et al., 1997; Maddox et al., 1997; Ravikovitch et al., 2000; Ravikovitch et al., 2001) and density functional theory (DFT) (Lastoskie et al., 1993; Olivier, 1995; Neimark et al., 1998; Neimark and Ravikovitch, 2001; Ravikovitch et al., 2001; Ravikovitch and Neimark, 2001). Both methods are in agreement with each other and with classical approaches like that of Broekhoff and de Boer for pores wider than 7 nm (Neimark and Ravikovitch, 2001). The appearance of highly ordered mesoporous adsorbents like MCM-41 with controlled pore size independently determined by the X ray diffraction method has played an important role in the justification of the molecular approaches. Nevertheless, some features of the hysteresis phenomenon are not comprehensively explained so far. The hysteresis loop is wider than that theoretically predicted, and the reversible part of the isotherm is markedly longer compared to the result obtained by the theories. It is natural to explain this contradiction by overcoming a potential barrier between the metastable adsorption branch of the isotherm and the equilibrium desorption branch corresponding to complete filling of the pore volume (Neimark and Vishnyakov, 2000; Vishnyakov and Neimark, 2003). The pore filling occurs via formation of bridges, which was not systematically considered by means of DFT. So far the DFT has been mainly applied to systems with homogeneous density distribution in two directions. Our aim is to adapt the DFT to cylindrical pores accounting for the

*To whom correspondence should be addressed.

density distribution along the radial and axial directions. It will allow us to consider the mechanism of condensation and evaporation in finite and infinite pores in canonical ensemble and the mechanism of nucleation by grand canonical version of the two dimensional DFT.

Model

We use the Tarazona's formulation of the smoothed density approximation (Tarazona, 1985), the Carnahan—Starling equation of state (CS EOS) for the equivalent hard sphere fluid (Carnahan and Starling, 1969) and the Weeks—Chandler—Andersen (WCA) scheme for the intermolecular interactions (Weeks et al., 1971). The WCA scheme is also used for calculation of the attractive fluid—solid potential, which is justified with reference to amorphous silica-like solids providing quantitative description of nitrogen and argon isotherms on non-porous silica at their boiling points. The latter is important condition of reliable prediction of the isotherms in cylindrical pores of different diameters having the same surface chemical structure as that of the reference non-porous solid. In order to account for the density distribution along radial and axial directions we divided corresponding coordinates into equal segments having thickness of one tenth of the collision diameter, so that the fluid and the solid were represented by a set of concentric rings. The mass of such a ring inside the pore is proportional to the fluid density at given radius and z-coordinate. The 3-parametric discrete set of Tarazona's weighted functions and that of WCA potentials were defined for each pair of rings as a function of their radii and the difference of z-coordinates. The density profile is determined by minimization of the grand thermodynamic potential in grand canonical ensemble and by minimization of the Helmholtz free energy in canonical ensemble.

Discussion

In this section we present some results for calculation of argon adsorption in cylindrical pores of MCM-41 adsorbents at 87.3 K. To model infinitely long pore we used a simulation cell of 25 collision diameters. Boundary conditions on the two cross sections were defined as mirror images. In the case of finite pore we accounted for the outer flat surface of infinite extent, which was modeled by the circle having radius 15 collision diameters with mirror image on the boundary. The cell included the segment under the flat outer surface surrounding the pore entrance having width of 5 times the collision diameter. The adsorption mechanism was investigated in canonical and grand canonical ensemble.

Canonical Ensemble for Infinite Cylindrical Pore

The canonical version of DFT is destined to the analysis of adsorption in pores with specified amount adsorbed. The iteration procedure of minimization of the Helmholtz free energy is described in our previous paper (Ustinov and Do, 2003). In order to provoke nucleation and cavitation in the proximity of corresponding spinodal points a small surface heterogeneity was introduced. An example of argon adsorption isotherm is shown in Fig. 1.

The equilibrium transition pressure ($p/p_0 = 0.42$) corresponds to vertical line *BH*. The section *BCD* is the metastable adsorption branch. At the vapor-like spinodal point *D* the adsorbed phase splits into two sections separated by a semispherical meniscus. The pressure jumps to the equilibrium transition pressure (point *E*) and remains constant with further increase of the amount adsorbed. The vapor-like section shrinks up to small bubble, which eventually looses its stability in the point *F* followed by its disappearance and the formation of the continuous liquid-like phase. The pressure jumps to the point *G*, corresponding to the stretched liquid. Further increase of amount adsorbed leads to the increase of the bulk pressure. During desorption in canonical ensemble the isotherm for the first period goes along the curve *MLHGN*. At the

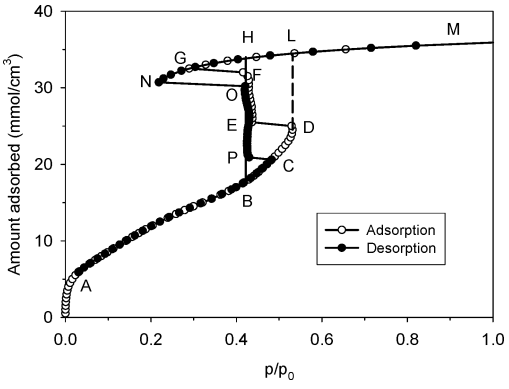

Figure 1. Argon adsorption isotherm in cylindrical pore of 4 nm diameter at 87.3 K.

liquid-like spinodal point N the adsorbed phase represents the mostly stretched liquid. The hydrostatic pressure at the pore axis is -314 atmospheres, which is exactly the minimal pressure on the pressure—density dependence obtained by the CS EOS combined with the WCA equation for homogeneous argon at 87.3 K. Thus, a small decrease in the adsorbed average density leads to the break of the adsorbed phase and its split into the liquid-like and the vapor-like sections separated by the semispherical meniscus. In the range between points O and P the vapor—liquid coexistence occurs at nearly constant pressure coincided with the equilibrium transition pressure.

In the point P the liquid-like phase presents a relatively thin bridge having width about 5 collision diameters, which is the limiting case of its mechanical stability. The decrease of its thickness immediately leads to its disappearance with the formation of the liquid film homogeneously distributed along the pore axis.

Canonical Ensemble for Finite Cylindrical Pore

We now turn our attention to finite pores. Figure 2 shows the density distribution in the vicinity of the entrance of cylindrical pore of 4 nm in the form of contour lines. The contour lines correspond to constant values of the reduced density $\rho\sigma_{ff}^3$ within the range from 0 to 1 with an increment of 0.1.

Figure 2(a) corresponds to the vapor—liquid coexistence at the pressure, which is very close to the equilibrium transition pressure. While Fig. 2(b) shows the liquid film just after the evaporation of the liquid argon from the core of the pore. In the range of the amount adsorbed where the vapor-like and the liquid-like phases are in coexistence the adsorption and desorption branches of the isotherm are exactly reversible at the equilibrium transition pressure. It corroborates the classical scenario that the capillary evaporation occurs at equilibrium transition pressure, while the adsorption branch passes through the vapor-like spinodal point. If the pore is long enough and is considered as an open system (grand canonical ensemble), the adsorption branch is *ABCDLM*, and desorption branch of the isotherm is *MLHBA*. Hence, the hysteresis loop is represented by the closed curve *BCDLHB*. However, the comparison of the theoretical result with experimental data reveals some disagreements. The width of the experimental hysteresis loop is markedly less than that predicted by the DFT, and the reversible part of the isotherm is longer than that predicted by the theory. It may be explained by the possibility of overcoming the potential barrier during adsorption at a lower pressure than the vapor-like spinodal point. This phenomenon cannot be investigated in canonical ensemble, since the pressure of the vapor—liquid coexistence is very close to the equilibrium transition pressure even in the limiting case of the smallest mechanically stable bridge. It means that in the canonical ensemble we are not able to vary the pressure in the region between the equilibrium transition point and the vapor-like spinodal point, which makes us to turn to the grand canonical version of the 2D DFT.

Grand Canonical Ensemble for Infinite Cylindrical Pore

If the bulk pressure is less than that for the spinodal point there is a potential barrier, which separates the local and global minima of the grand thermodynamic potential. Thus, despite the complete filling of the pore is

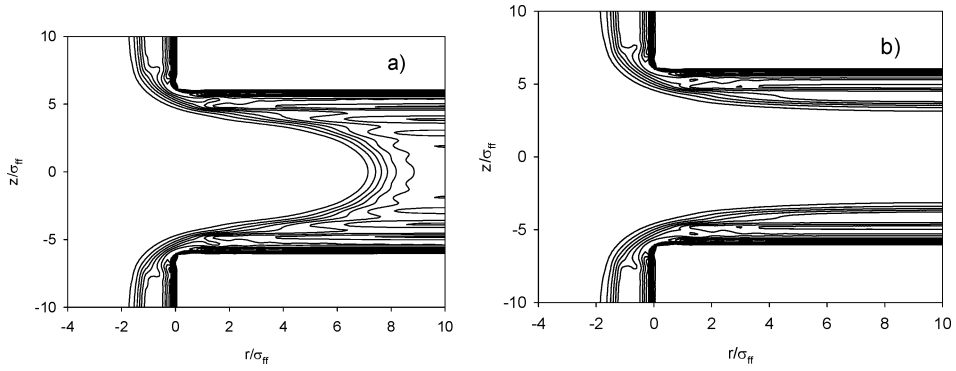

Figure 2. Density distribution during capillary evaporation of argon from the finite pore of 4 nm diameter. p/p_0 (a) 0.434; (b) 0.495.

thermodynamically favorable at pressures higher than the equilibrium transition pressure, the potential barrier could prevent the capillary condensation to occur. Such a barrier may be overcome due to the density fluctuations, surface roughness or the energetic heterogeneity. In all cases the spontaneous pore filling starts from the appearance of a nucleus. We proceed from the assumption that the mechanism of the nucleation is not crucial in terms of the form of the potential barrier. It allows us to use an external potential field in the form of the Gaussian function:

$$u^{ext} = \frac{\lambda}{\sqrt{2\pi}\delta} \exp[-(z - z_0)^2/(2\delta^2)] \qquad (1)$$

The only requirement is that the standard deviation δ should be sufficiently small. Here we used the value of one collision diameter. Imposing of the external potential field leads to the rearrangement of the density distribution in the vicinity of the coordinate z_0, which is associated with the work to be done for such a rearrangement. This work is attributed to the potential barrier and calculated as the difference between interaction potentials of the adsorbed fluid with the external field before the rearrangement has started (homogeneous axial distribution) and after the establishment of equilibrium state. The critical potential barrier that provokes the spontaneous pore filling is determined by tuning of the multiplier λ in Eq. (1).

The critical density distribution at $p/p_0 = 0.45$ just before the capillary condensation of argon in the pore having diameter 4 nm is presented in Fig. 3.

It is seen from the figure that the critical nucleus has the form of bump rather than bridge, which is confirmed by a number of investigators (see Vishnyakov and Neimark, 2003 for the review). The density in the pore center is only 0.314 mmol/cm^3, which is about 110 times less than the density of liquid argon. Right plot in the figure presents the dependences of the potential barrier on the bulk pressure for different pore diameters. It is unknown exactly what is the smallest barrier, which could be overcome due to the density fluctuations. However, since the argon adsorption isotherm is reversible for the pore diameter of 3.54 nm, one can suggest that it exceeds 20 kT. Let this critical barrier be of 22 kT (dashed line in the figure). In this case the point of intersection of the dashed line and a descending curve corresponds to the condensation pressure.

Some Unresolved Problems

The appearance of highly ordered mesoporous materials like MCM-41 gave an excellent opportunity to check different theories, since the pore diameter may be independently determined by XRD method. Some experimental data are generalized in Fig. 4. Prediction of the adsorption isotherm in the pore of known diameter requires knowledge of the specific surface area of a reference nonporous system having the same chemical structure. This is because the molecular parameters for the solid—fluid interaction may be determined by tuning them to provide the best fit of experimental data for the nonporous solid. Unfortunately, the BET surface area is extremely uncertain. It allows us to use the surface area as an additional adjusting parameter. We relied on N_2 and Ar adsorption isotherms at their boiling points on amorphous silica LiChrospher Si-1000 (Jaroniec and Kruk, 1999; Kruk and Jaroniec, 2000).

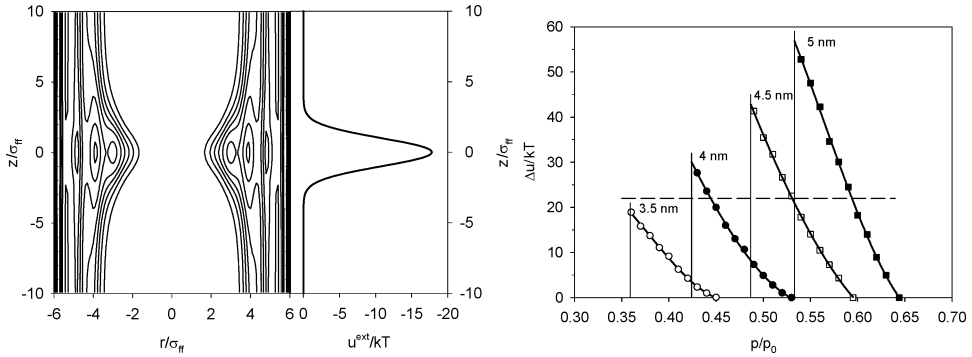

Figure 3. Nucleation induced by the external field. (Left plot) the density distribution at $p/p_0 = 0.45$ and $D = 4$ nm before the condensation. (Right plot) the dependence of the potential barrier on the bulk pressure. The pore diameter (nm): (○) 3.54, (●) 4.0, (□) 4.53, (■) 5.0. Vertical lines correspond to equilibrium transition pressures.

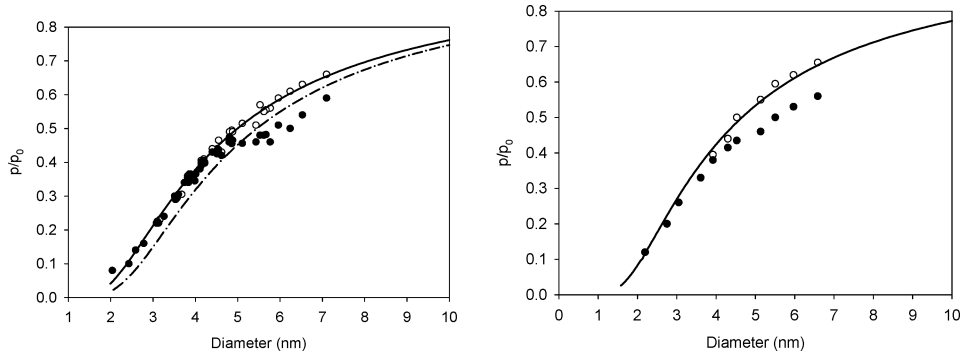

Figure 4. The dependence of condensation pressure (open circles) and evaporation pressure (filled circles) on the pore diameter. Left plot: N_2 adsorption in MCM-41 at 77 K (Kruk and Jaroniec, 2001). Right plot: Ar adsorption at 87.3 K (Kruk and Jaroniec, 2000). Explanations are in the text.

We found that the experimental dependence of the condensation pressure on the pore diameter may be fitted only by the theoretical dependence obtained for the equilibrium transition pressures. Fig. 4 presents these fits for N_2 and Ar.

Solid lines are calculated by the DFT as equilibrium transition curves in case of the specific surface area of nonporous silica equals to 24 m^2/g. Note that this surface area is the same for nitrogen and argon adsorption, which provides the self-consistency of the approach. The dash-dotted line is plotted for the surface area of 19.65 m^2/g. Thus, the variation of the surface area just shifts the curve along the pressure axis, which makes impossible to match this curve with the experimental evaporation pressure—diameter dependence. Similarly, the dependence of pressure for spinodal points on diameter by no means could be matched with the adsorption branches of the isotherms. What it means is that the capillary condensation seems to occur at true equilibrium, while the metastable state on desorption branch precedes the capillary evaporation. Such a mechanism is not supported by the classical scenario and cannot be explained in the framework of the simplest molecular model used in the DFT and molecular simulations. Further investigations are required.

Conclusion

A version of the non-local density functional theory accounting for the density distribution along the radial and axial directions is an effective tool for analysis of adsorption in cylindrical pores, mechanism of capillary condensation and evaporation, nucleation and cavitation. We showed that the nucleation is associated with the formation of bumps rather than bridges. Application of the approach to finite pores has confirmed the classical scenario of equilibrium evaporation. Nevertheless, experimental data seems to show that the adsorption branch of the isotherm is very close to the true equilibrium. Further investigations are needed.

Acknowledgments

Support from the Australian Research Council is gratefully acknowledged. The authors are grateful to Dr. Mietek Jaroniec for the experimental data and discussion.

References

Jaroniec, M. and M. Kruk, "Standard Nitrogen Adsorption Data for Characterization of Nanoporous Silicas," *Langmuir*, **15**, 5410–5413 (1999).

Kruk, M. and M. Jaroniec, "Accurate Method for Calculating Mesopore Size Distributions from Argon Ddsorption Data at 87 K Developed using Model MCM-41 Materials," *Chem. Mater.*, **12**, 222–230 (2000).

Kruk, M. and M. Jaroniec, "Gas Adsorption Characterization of Ordered Organic—Inorganic Nanocomposite Materials," *Chem. Mater.*, **13**, 3169–3183 (2001).

Lastoskie, C., K.E. Gubbins, and N. Quirke, "Pore Size Heterogeneity and the Carbon Slit Pore: A Density Functional Theory Model," *Langmuir*, **9**, 2693–2702 (1993).

Neimark, A.V. and P.I., Ravikovitch, "Capillary Condensation in MMS and Pore Structure Characterization," *Microporous Mesoporous Mater.*, **44/45**, 697–707 (2001).

Neimark, A.V., P.I. Ravikovitch, M. Grün, F. Schüth, and K.K. Unger, "Pore Size Analysis of MCM-41 Type Adsorbents By Means of Nitrogen and Argon Adsorption," *J. Colloid Interface Science* , **207**, 159–169 (1998).

Neimark, A.V. and A. Vishnyakov, "Gauge Cell Method For Simulation Studies of Phase Transitions in Confined Systems,"*Phys. Review E*, **62**, 4611–4622 (2000).

Maddox, M.W., J.P. Olivier, and K.E. Gubbins, "Characterization of MCM-41 Using Molecular Simulation: Heterogeneity Effects,"*Langmuir*, **13**, 1737–1745 (1997).

Olivier, J.P. "Modeling Physical Adsorption on Porous and Nonporous Solids Using Density Functional Theory," *J. Porous Mater.*, **2**, 9–17 (1995).

Ravikovitch, P.I. and A.V. Neimark, "Characterization of Nanoporous Materials from Adsorption and Desorption Isotherms," *Colloids and Surfaces A: Physicochem. Eng. Aspects.*, **187**/**188**, 11–21 (2001).

Ravikovitch, P.I., A. Vishnyakov, and A.V. Neimark, "Density Functional Theories and Molecular Simulations of Adsorption and Phase Transitions in Nanopores," *Phys. Review E*, **64**, 011602 (2001).

Ravikovitch, P.I., A. Vishnyakov, R. Russo, and A.V. Neimark, "Unified Approach to Pore Size Characterization of Microporous Carbonaceous Materials from N_2, Ar, and CO_2 Adsorption Isotherms," *Langmuir*, **16**, 2311–2320 (2000).

Suzuki, T., K. Kaneko, and K.E. Gubbins, "Pore Width-Sensitive Filling Mechanism for CCl_4 in a Graphitic Micropore by Computer Simulation," *Langmuir*, **13**, 2545–2549 (1997).

Tarazona, P., "Free Energy Density Functional for Hard Sphere," *Phys. Rev. A.*, **31**, 2672–2679 (1985).

Ustinov, E.A. and D.D. Do, "Application of Density Functional Theory to Capillary Phenomena in Cylindrical Mesopores With Radial and Longitudinal Density Distributions," *J. Chem. Phys.*, **120**, 9769–9781 (2004).

Vishnyakov, A. and A.V. Neimark, "Nucleation of Liquid Bridges and Bubbles in Nanoscale Capillaries," *J. Chem. Phys.*, **119**, 9755–9764 (2003).

Carnahan, N.F. and K.E. Starling, "Equation of State for Non-Attracting Rigid Sphere," *J. Chem. Phys.*, **51**, 635–636, (1969).

Weeks, J.D., D. Chandler, and H.C. Andersen, "Role of Repulsive Forces in Determining the Equilibrium Structure of Simple Liquids," *J. Chem. Phys.*, **54**, 5237–5247 (1971).